

University of Mississippi

eGrove

Faculty and Student Publications

Engineering, School of

1-1-2021

“Greener” chemical modification of cellulose nanocrystals via oxa-Michael addition with N-Benzylmaleimide

Mohammad Jahid Hasan
University of Mississippi

Ashley E. Johnson
University of Mississippi

Esteban E. Ureña-Benavides
University of Mississippi

Follow this and additional works at: https://egrove.olemiss.edu/engineering_facpubs

 Part of the [Chemical Engineering Commons](#)

Recommended Citation

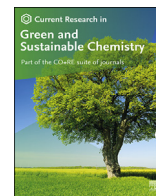
Hasan, M. J., Johnson, A. E., & Ureña-Benavides, E. E. (2021). “Greener” chemical modification of cellulose nanocrystals via oxa-Michael addition with N-Benzylmaleimide. *Current Research in Green and Sustainable Chemistry*, 4, 100081. <https://doi.org/10.1016/j.crgsc.2021.100081>

This Article is brought to you for free and open access by the Engineering, School of at eGrove. It has been accepted for inclusion in Faculty and Student Publications by an authorized administrator of eGrove. For more information, please contact egrove@olemiss.edu.

Contents lists available at [ScienceDirect](https://www.sciencedirect.com)

Current Research in Green and Sustainable Chemistry

journal homepage: [www.elsevier.com/journals/
current-research-in-green-and-sustainable-chemistry/2666-0865](https://www.elsevier.com/journals/current-research-in-green-and-sustainable-chemistry/2666-0865)



“Greener” chemical modification of cellulose nanocrystals via oxa-Michael addition with N-Benzylmaleimide



Mohammad Jahid Hasan^{a,b}, Ashley E. Johnson^a, Esteban E. Ureña-Benavides^{a,b,*}

^a Department of Chemical Engineering, University of Mississippi, University, MS, 38677, USA

^b Department of Biomedical Engineering and Chemical Engineering, The University of Texas at San Antonio, San Antonio, 78249, TX, USA

ARTICLE INFO

Keywords:

Cellulose nanocrystals (CNC)
Surface modification
Oxa-Michael addition
Etherification
Thermal stability
Green chemistry principles

ABSTRACT

Surface modification of cellulose nanocrystals (CNCs) was conducted by an oxa-Michael addition of primary hydroxyl groups on the CNC surface with N-Benzylmaleimide (BnM). Six principles of green chemistry were used to obtain the hydrophobized CNC. Two catalytic approaches were used, a self-catalyzed reaction where alkyl sulfuric acid on the surface of the CNC was the catalyst, and a base-catalyzed approach using triethylamine (TEA). DMSO was chosen as reaction solvent due to its low cost, low toxicity and ability to disperse native CNC compared to other polar diprotic solvents. NMR and FTIR studies confirmed the successful modification of CNCs in both reaction routes. The TEA-catalyzed reaction showed a higher BnM conversion at 70 °C after 72 h (46 ± 2%) compared to the self-catalyzed reaction at 100 °C (24 ± 2%). Since BnM was added at a two-fold excess compared to superficial primary –OH groups, these had estimated conversions of 92% and 48%, for the base catalyzed and acid catalyzed routes, respectively. Zeta potential measurements suggest, the sulfate groups were retained after the modification reaction. AFM demonstrated no change in particle morphology after modification. Modified CNCs degraded at a higher temperature (390 ± 8 °C) when the reaction was catalyzed by TEA compared to native CNCs and the self-catalyzed product (220 ± 10 °C). Contact angle measurements demonstrated the increased hydrophobicity of the modified nanoparticles. Visual inspection and UV–vis spectroscopy demonstrated the modified CNCs had an increased affinity towards organic solvents like acetone, acetonitrile and toluene.

1. Introduction

Cellulose Nanocrystals (CNC), extracted by the acid hydrolysis of plants cellulose, have received significant attention in the last two decades for their light-weight, large axial Young's modulus and limited toxicity [1–3]. They also have the benefits of being biobased and biodegradable [4,5]. These advantages of the CNCs can be utilized in a wide range of applications such as the development of bio-nanocomposites [5,6], water treatment methods [7], controlled-drug delivery vehicles [8], emulsion [9,10], and papers coatings [11]. The surface of CNCs can be modified and then used in applications in extreme environments such as solar cells [12], CNC-reinforced polymer nanocomposites [13], and high-temperature enhanced oil recovery [14], where a high thermal and chemical stability of the nanoparticles is required.

The surface of a CNC is covered with hydroxyl groups, which make them highly hydrophilic. Typically, they are isolated through sulfuric acid hydrolysis, which converts approximately 30% of the available

primary hydroxyl groups on the surface into sulfates [15,16]. Sulfates are easily deprotonated in aqueous media resulting in stable negatively charged CNC. The hydrophilicity of the CNC surface hinders its dispersion in organic polymers and solvents. Several methods have been studied in literature to disperse unmodified (pristine) CNC in an organic media. Firstly, a solvent-exchange sol-gel technique, where a dipolar organic solvent is added to a CNC aqueous suspension, leading to the gelation of the mixture. The produced organogel is then immersed into a solution to imbibe a polymer into the CNC network [17,18]. This method can improve the mechanical properties in the rubbery state by formation of a percolation network but is not expected to be effective below the percolation threshold. Moreover, nanocomposites of styrene butadiene rubber filled with CNCs through the sol-gel technique showed to be less efficient in improving mechanical properties than those prepared by solution casting and compression molding [19]. Even though dispersion of unmodified CNCs in a hydrophobic polymer matrix is possible by controlling the processing conditions, this approach does not contribute to improving stress transfer from the polymer to the nanocrystals. Surface

* Corresponding author. Department of Chemical Engineering, University of Mississippi, University, MS, 38677, USA.

E-mail address: esteban.urena-benavides@utsa.edu (E.E. Ureña-Benavides).

<https://doi.org/10.1016/j.crgsc.2021.100081>

Received 24 September 2020; Received in revised form 1 March 2021; Accepted 9 March 2021

Available online 23 March 2021

2666-0865/© 2021 The Author(s). Published by Elsevier B.V. This is an open access article under the CC BY license (<http://creativecommons.org/licenses/by/4.0/>).

modification would be required for that purpose to achieve reinforcement at concentrations below the percolation threshold.

Several methods of modification have been explored to disperse CNCs in various solvents and polymer matrices. Modifications include several “grafting from” atom transfer radical polymerization (ATRP) reactions to introduce poly (N,N-dimethylaminoethyl methacrylate) (PDMAEMA), poly (acrylic acid) (PAA), polystyrene (PS), and ring opening polymerizations to graft poly (lactic acid) (PLA), poly (caprolactone) (PCL), etc. [3, 20, 21]. Polymers grafted to CNC include poly (ethylene glycol) (PEG), poly (caprolactone) (PCL), maleated polypropylene (PPgMA), among others [3, 20]. Small molecules have also been introduced onto the surface of CNCs via oxidations [22], silylations [23], sulfonations [24], acetylations [25], esterifications [26], etherifications [27], and amidations [28]. More recently, aldehyde-modified CNCs and hydrazine-modified CNCs were prepared to fabricate CNC crosslinked hydrogels [29].

Current literature of CNC modifications typically pays little attention to the colloidal stability of the nanoparticles during surface modification. Often CNCs are partially aggregated, leading to unexposed surfaces not available for modification. Surface coverages are often presented, but yields are rarely mentioned; both of these variables can be affected by the colloidal stability of the CNCs during modification. Another drawback of current modification schemes is the use of toxic or unstable chemicals like isocyanates and acyl chlorides. Anhydrides are also commonly used for acylation reactions, but they require anhydrous reaction conditions as they hydrolyze easily. Silylation reactions produce highly unstable alkoxy silane linkages, which are readily hydrolyzed, limiting its applicability. Ester groups are also easily cleaved at elevated temperatures, especially in the presence of water. ATRP requires a preliminary bromination reaction to introduce the initiator on the CNC surface; the reaction is highly exothermic and can potentially cause CNC degradation [3, 20, 30].

In this work, acid-catalyzed and base-catalyzed oxa-Michael addition reactions were tested, for the first time, to graft N-Benzylmaleimide (BnM) onto the CNC surface. The modification of the CNC surface was performed through ether linkages, which are thermally and chemically stable. Oxa-Michael additions are usually catalyzed by bases [31, 32]; however, Brønsted acid catalysis has been reported with strong acids like o-benzenedisulfonamide [33], bis(trifluoromethanesulfon) imide (Tf₂NH) [34], trifluoromethanesulfonic [35], methanesulfonic acid [35], and p-toluenesulfonic acid monohydrate (TsOH·H₂O) [35]. Herein, the oxa-Michael reaction was self-catalyzed by the alkyl sulfuric acid groups on the nanocrystals themselves. Additionally, triethylamine was also used as a catalyst in a base-catalyzed oxa-Michael addition reaction. Grafting of maleimide to the CNC surfaces was achieved by following 6 of the 12 green chemistry principles, i.e., atom economy, less hazardous chemical synthesis, designing safer chemicals (products), use of renewable feedstocks, reduced derivatives, and inherently safer chemistry for accident prevention [36]. The modified hydrophobic CNCs herein obtained can be used in a variety of applications where thermal or chemical stability are required, in addition to partial hydrophobization [37]. Examples are stabilizing Pickering emulsions [38, 39], preparation of thermoset polymer nanocomposites [5, 17, 40], enhanced oil recovery [41], and underground sequestration of CO₂ [42].

2. Materials and methods

2.1. Materials

Southern bleached softwood Kraft (SBSK) pulp was kindly donated by Weyerhaeuser pulp mill (Columbus, MS) as a cellulosic source for the synthesis of CNC. Sulfuric acid (>96% purity), Dimethyl Sulfoxide (>99.9% purity), Acetone (>99%), Acetonitrile (>99.9%), Propylene carbonate (>99.5%), N-Benzylmaleimide (>99%), Trimethylamine (>99%), Dimethyl sulfone, Deuterated DMSO (>99.9%), Heptane (>99%) and Toluene (>99.9%) were all purchased from Fisher Scientific and used as received.

2.2. Isolation of cellulose nanocrystals (CNC)

The hydrolysis reaction of cellulosic wood pulp and sulfuric acid was done as reported in multiple articles [15, 16, 43]. At first, 840 ml of 64% sulfuric acid was added to the beaker, followed by the addition of 48 g of SBSK pulp. The reaction was run for 50 min at 45 °C with stirring at 230–240 rpm. Upon completion, the reaction mixture was diluted 10-fold with cold deionized water in a 10 L beaker and was left overnight to precipitate the cellulose. A large portion of excess acid in the CNC suspension was removed by decanting the comparatively clear acidic water from the top of the beaker. The remaining acid was removed by centrifugation of the residual CNC suspension. The supernatant was removed, and the centrifuged sludge was further washed with DI water by using 3.5 kDa RC dialysis membranes for several days to remove all excess acid. The dialyzed CNC dispersion was then sonicated by an ultrasonic horn (Qsonica; Q700) to disperse the CNC and was then stored. Safety note: concentrated sulfuric acid is extremely corrosive and can cause serious burns; it is recommended to be used in a fume hood with rubber apron, gloves and boots, and a face shield over the chemical safety goggles.

2.3. Dispersion of CNCs in various solvents

The CNC dispersion was first freeze dried in a FreeZone 6 L labconco (Kansas City, MO) freeze dryer. Then 10 mg of freeze-dried samples were dispersed in 10 ml solvent and sonicated by using an ultrasonic horn (Qsonica, Q700, Newtown, CT). Dispersibility of neat CNCs in Deionized Water, and several aprotic dipolar organic solvents like dimethyl sulfoxide (DMSO), acetone, acetonitrile, and propylene carbonate (PC) was observed by visual inspection of the dispersions and by monitoring the UV-visible spectra with a Genesys 150 UV-Visible spectrophotometer (Thermo Scientific, Waltham, MA) within the wavelength of 200 nm–800 nm at 0 h and after 24 h.

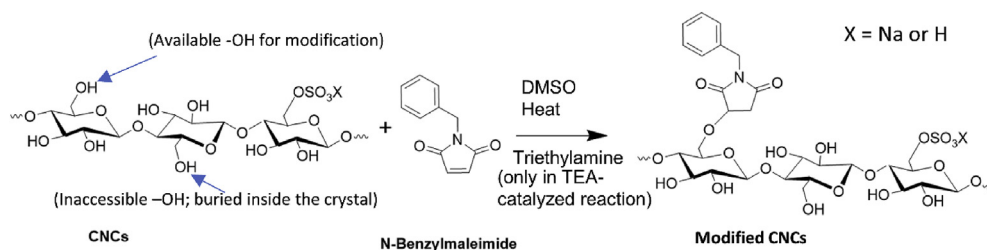
2.4. Modification of CNCs by oxa-Michael addition reaction

In the case of self-catalyzed oxa-Michael addition reaction (Scheme 1), the alkyl sulfuric acid on the CNCs themselves was utilized as a catalyst for the reaction. The amount of sulfur on the CNCs surface was determined by a conductometric titration following a method described by Abitbol et al. [44] and presented in supporting information (Fig. S1). The sulfur content in CNC was calculated to be $0.42 \pm 0.5\%$ (g-sulfur/100 g-cellulose). In short, 1.64 g of freeze-dried CNC was dispersed in 100 ml dimethyl sulfoxide (1 v/v%) and sonicated using an ultrasonic horn (Qsonica, Q700, Newtown, CT) until a stable dispersion was achieved. The dispersion was transferred to a round bottom flask and then 0.412 g (0.0022 mol) of N-Benzylmaleimide (BnM) was added. The mixture was then heated to 70 °C and the reaction was run for 72 h with stirring. Upon completion, the reaction was cooled down to room temperature, and freeze-dried. The dried product was then washed with toluene (twice) and then heptane (twice) to remove the unreacted BnM. The purified product was then dried and stored for further analysis.

In the case of TEA-catalyzed oxa-Michael addition reaction, the pH of the raw CNCs suspension was adjusted to 7 before freeze-drying. The freeze-dried CNCs were then used in the TEA-catalyzed modification reaction. The procedure was the same as self-catalyzed reaction except for the addition of 30 μ L triethylamine (0.1 equivalents of BnM) to the reaction mixture as a basic catalyst.

2.5. Fourier transform infrared (FTIR) spectroscopy

Fourier transform infrared (FTIR) spectra of CNC samples were recorded on a Cary 630 FTIR spectrometer (Agilent Technologies, Santa Clara, California). A low amount (approximately 10 mg) of freeze-dried CNC samples were tested in attenuated total reflectance (ATR) sampling mode at a resolution of 4 cm⁻¹ with the spectrum range of



Scheme 1. Oxa-Michael addition reaction of cellulose nanocrystals with BnM.

4000–600 cm^{-1} .

2.6. Calculation of conversions

The conversions of the modification reactions were obtained by tracking the disappearance of BnM over time with a 300 MHz ^1H proton NMR (Bruker Avance-300, Bruker, Billerica, MA). For NMR analysis, all the modification reactions were done in small scales in closed vials; 5 ml of DMSO- d_6 was used instead of regular DMSO and 0.010 g dimethyl sulfone was added as an internal standard. The other chemicals were used proportionately. Around 0.5 ml of the reaction mixtures were sampled at time 0 h, 24 h, 48 h, and 72 h and transferred to NMR tubes to be analyzed. The conversions were calculated from the decrease of specific peaks of BnM in NMR spectra according to equation (1).

$$\text{BnM Conversion (\%)} = \frac{I_0 - I_T}{I_0} \times 100\% \quad (1)$$

Where, I_0 = Integral of BnM peak (A) at time 0 h, and, I_T = Integral of BnM peak (A) at time T. Both integrals were normalized to maintain a constant peak area of the internal standard.

2.7. Atomic force microscopy (AFM)

A drop of dilute CNC suspensions (0.0001 wt%) was dried onto a freshly cleaved mica surface (1.5 cm^2 , Ted Pella, Inc.) and imaged using an atomic force microscope (MultiMode 8, Bruker Nano, Inc.) in tapping mode. Both the neat CNCs and the modified CNCs were imaged with the AFM, and their morphology was compared to see if there was any change in the structure after modification. At least 100 nanocrystals were analyzed from each sample by using the software Gwydion (version 2.55), and the size distributions were plotted.

2.8. Thermal gravimetric analysis (TGA)

Thermogravimetric Analysis (TGA) of CNC samples was performed with a thermogravimetric analyzer (Q500, TA Instruments). The dry CNC samples (5–10 mg) were heated on a platinum pan from room temperature up to 600 $^\circ\text{C}$ under nitrogen at 10 $^\circ\text{C}/\text{min}$ while collecting the weight as a function of temperature.

2.9. Zeta potential measurement

Zeta potential of CNC samples was obtained with a Malvern Zetasizer Nano ZS (Malvern Instruments, UK). Aqueous suspensions of the CNC were diluted to 0.1 wt% (1 mg/ml) and its pH adjusted to pH 7 with HCl or NaOH, then added to the disposable zetasizer cells to measure the zeta potential.

2.10. Contact angle measurement

The contact angles of CNCs and modified CNCs were obtained at room temperature (22 $^\circ\text{C}$) by using a Krüss Tensiometer DSA100E (Krüss, Hamburg, Germany), operating high resolution camera and a motorized

syringe (0.508 mm in outer diameter). At first, 1 wt% (10 mg/ml) aqueous suspensions of CNC samples (100 μL) were dropped on mica sheets (Highest Grade V1 Mica Discs, 12 mm, Ted Pella Inc., Redding, CA, United States) and dried in a desiccator to form CNC films. Water, ethylene glycol (EG) and diiodomethane (DIM) were used as probe liquids. Contact angle measurements were performed via static sessile drop shape analysis, whereas the droplet size was 5 μL in all measurements. A video was recorded immediately after the droplet was deposited on the substrate and the measurements were taken after 5 s by using the video footage.

3. Results and discussions

3.1. Solvent selection

The modification reactions had to take place in a dipolar aprotic organic medium since excessive water may interfere with the surface modification reaction, although anhydrous conditions are not necessary. CNCs from sulfuric acid hydrolysis are highly stable in water, and only a few dipolar aprotic solvents have been used to stabilize their dispersions successfully [45]. Freeze-dried CNCs were transferred into acetone, acetonitrile (ACN), DMSO, and Propylene Carbonate (PC). They have high dielectric constants (ϵ) of 20.7 (Acetone), 36.64 (ACN), 47.24 (DMSO), and 66.14 (PC) [46]. In general, higher dielectric constants are correlated to greater polarity. From the visual inspection of the CNCs dispersions and respective UV–vis spectroscopy at time 0 h and 24 h (Fig. 1), DMSO was found to be the best organic solvent among them to make stable CNC dispersions. Negligible precipitation was observed in DMSO after 24 h (Fig. 1b) with a minimal decrease of absorbance over time (Fig. 1d). In the case of propylene carbonate, there was little precipitation over the time and, whereas acetone and acetonitrile had more downfall, indicating less stable dispersions (Fig. 1e–f). The light absorbance of PC decreased over time, probably due to some precipitation, while for ACN it increased, possibly due to increased scattering caused by suspended CNC aggregates. Hence DMSO was chosen as the solvent for the modification reaction. DMSO has limited toxicity, and has been previously been used to disperse CNCs [3,21,45]. Other solvents that have been used to successfully disperse CNCs are N,N-dimethyl formamide (DMF), N-methyl pyrrolidone (NMP), formic acid and m-cresol; however, their use is herein discouraged due to their high toxicity [17, 45,47].

3.2. Modifications of CNCs by oxa-Michael addition reaction

Chemical modification of the CNCs was performed by reacting BnM with the primary hydroxyl groups on the cellulose surface according to the reaction in Scheme 1. The reaction viability can be explained by the poor electron density on the maleimide double bond and the high temperature. The amount of available primary $-\text{OH}$ groups for the modification reactions were obtained by following the procedure described by Shin et al. [40]. Each cellobiose has two hydroxyl groups on the CNC surface, but one hydroxyl group is oriented inside the crystal and not available for the reaction [3,6]. So, for each repeat unit on the surface of the CNC only one primary $-\text{OH}$ group is available. If that group is already

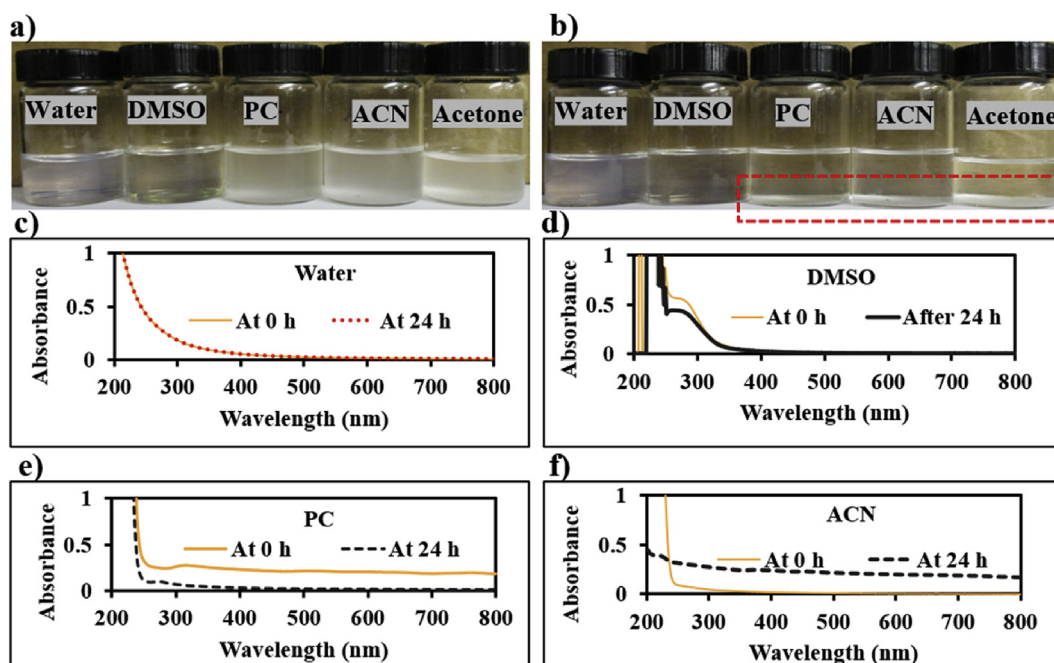


Fig. 1. Dispersibility of neat CNCs in DI water, DMSO, propylene carbonate (PC), acetonitrile (ACN), and acetone; (a) at 0 h; (b) after 24 h; UV-Visible spectra of CNCs dispersions in (c) water; (d) DMSO; (e) propylene carbonate (PC); (f) acetonitrile (ACN). The rectangular red box in Figure b displays the precipitation of CNCs after 24 h.

modified with sulfate, then it will not be available for modification with BnM. However, generally, only about 30% of the superficial repeat units are modified with sulfate groups. The remaining ones are available for modification. This was taken into account for the calculations of available $-OH$ groups for the modification of CNC with BnM and the amount of available $-OH$ group for the modifications was calculated to be 0.673 mmol OH/g CNCs [40]. In the case of the acid-catalyzed reactions, the reaction was self-catalyzed by the alkyl sulfuric acid groups on the nanocrystals themselves, which were generally present at a proportion of 1:2 with respect to the superficial primary $-OH$ [48]. The close proximity of the acidic groups to the Michael donor ($-OH$ group) may facilitate addition to the activated Michael acceptor (BnM). A two-fold molar excess of BnM was used with respect to the available primary $-OH$ to drive the reaction towards the products. Despite being present in an excess, the conversion is calculated in terms of BnM since its concentration is known with greater accuracy than the superficial $-OH$ groups.

The acid-catalyzed oxa-Michael addition reactions were run at 70 °C and 100 °C, while the base-catalyzed reaction was run at 70 °C. Triethylamine was used as the basic catalyst. Table 1 shows the BnM conversion of the reactions that were determined after analyzing the NMR spectra. The self-catalyzed reaction that took place at 100 °C showed a conversion of $24 \pm 2\%$ after 72 h (Fig. 2b), while the reaction at 70 °C demonstrated an even lower conversion ($10 \pm 3\%$). On the other hand, the base-catalyzed reaction at 70 °C was found to be comparatively faster

with a higher conversion rate ($46 \pm 2\%$) (Fig. 2d). It should be noted that since the BnM is added at an approximately 2-fold excess, the highest attainable conversion is close to 50%. An accurate determination of the superficial primary $-OH$ conversion was not possible; however, it is estimated to be approximately twice of the BnM.

The modification of CNCs was further evaluated by the FTIR study, where the chemical composition of neat CNCs and modified CNCs was investigated (Fig. 3). The neat CNCs, self-catalyzed modified CNCs, and TEA-catalyzed modified CNCs exhibited characteristic cellulose absorption peaks at 3334 cm^{-1} ($-OH$ stretching bonds), 2895 cm^{-1} (symmetric C-H stretching vibration), 1653 cm^{-1} ($-OH$ bending), 1427 cm^{-1} (asymmetric angular deformation of C-H), 1314 cm^{-1} ($-CH_2$ wagging), and 1052 cm^{-1} (asymmetrical C-O-C glycoside bonds), consistent with published papers [49,50]. Both types of modified CNCs showed an additional peak at 1772 cm^{-1} , which was absent in unmodified CNCs, corresponding to the C=O functional group that came from BnM attached to the CNCs. The intensity of the C=O peak was higher in the TEA-catalyzed CNCs than the self-catalyzed CNCs, pointing to the greater attachment of BnM to CNCs.

3.3. Morphology of neat CNCs and modified CNCs

AFM height images of neat CNCs and modified CNCs were obtained (Fig. 4), and their size distributions were determined (Fig. S2). The rod-

Table 1
BnM conversion of the oxa-Michael addition reactions.

Reaction Type	Temperature (°C)	Time (h)	BnM Conversion (%)	Estimated Primary $-OH$ Conversion
Self-catalyzed	70	24	5 ± 2	10
Self-catalyzed	70	48	8 ± 2	16
Self-catalyzed	70	72	10 ± 3	20
Self-catalyzed	100	24	12 ± 3	24
Self-catalyzed	100	48	20 ± 2	40
Self-catalyzed	100	72	24 ± 2	48
TEA-catalyzed	70	24	29 ± 4	58
TEA-catalyzed	70	48	40 ± 3	80
TEA-catalyzed	70	72	46 ± 2	92

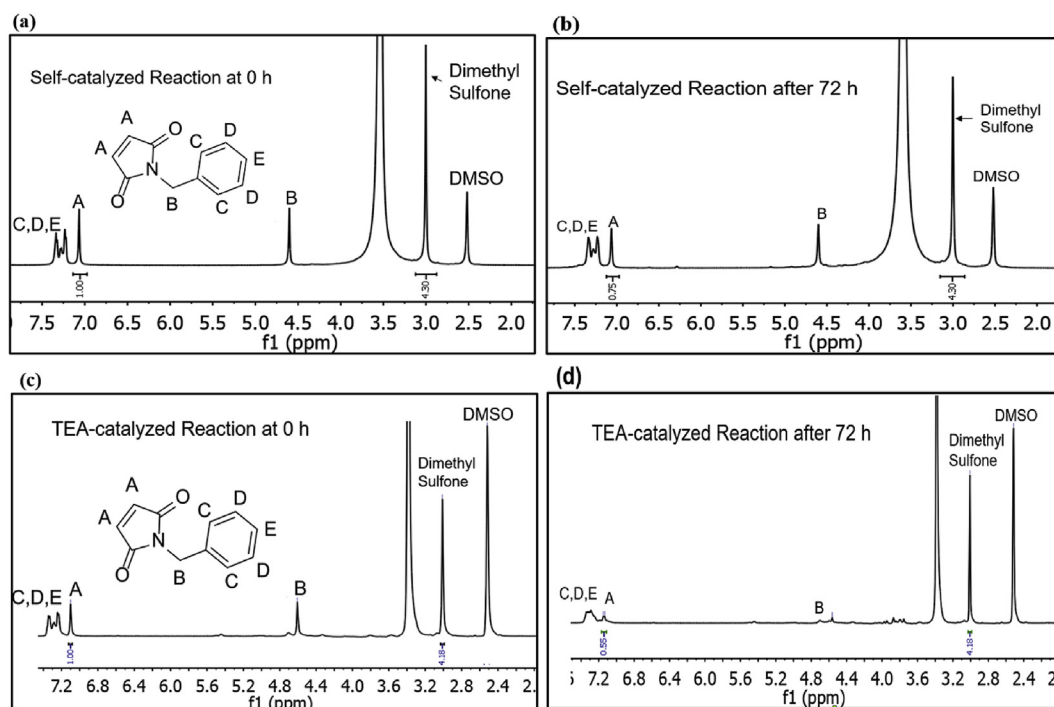


Fig. 2. NMR spectra of oxa-Michael addition reaction between BnM and cellulose nanocrystals of (a) self-catalyzed reaction (100 °C) at time 0 h; (b) self-catalyzed reaction (100 °C) after 72 h; (c) TEA-catalyzed reaction (70 °C) at time 0 h; (d) TEA-catalyzed reaction (70 °C) after 72 h.

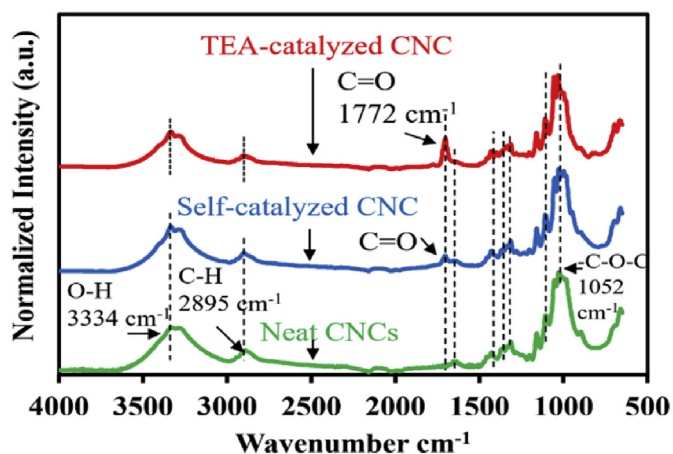


Fig. 3. FTIR spectroscopy of neat CNCs and modified CNCs showing the most relevant vibration peaks.

like neat CNCs were found to be dispersed well on the mica surface, whereas the modified CNCs were aggregated, probably due to the increased hydrophobicity of their surface. The average length of neat

CNCs was found to be 122 ± 67 nm, and the average height was 6.1 ± 3.1 nm. The average length and the average height of both self-catalyzed modified CNCs and the base-catalyzed modified CNCs remained almost the same as the neat CNCs, indicating no change in the morphology of the particles, which are essential for many applications such as making nanocomposites, coatings and controlled drug delivery.

3.4. Thermal stability of modified CNCs

The thermal decomposition of neat CNCs and modified CNCs was determined by TGA (Fig. 5a). All CNC samples initially lost weight in the range of 100 °C and 180 °C arising from the removal of moisture. The remaining weight loss occurred at 180 °C to 600 °C due to the degradation of cellulose chains. Derivative thermogravimetry (DTG) curve (Fig. 5b) showed that the rate of degradation for both neat CNCs and self-catalyzed modified CNCs peaked at 220 ± 10 °C, whereas both, neutral CNCs (freeze-dried at pH 7) and TEA-catalyzed CNCs, peaked at 290 ± 8 °C, indicating better thermal stability for the last two. Neat CNCs and self-catalyzed CNCs degraded at a lower temperature due to having acidic alyk sulfuric acid groups on their surface. On the contrary, neutral CNCs had comparatively higher thermal stability, consistent to published literature [51,52]. Since neutral CNCs were used in TEA-catalyzed reaction, the TEA-modified CNCs also had a higher thermal stability.

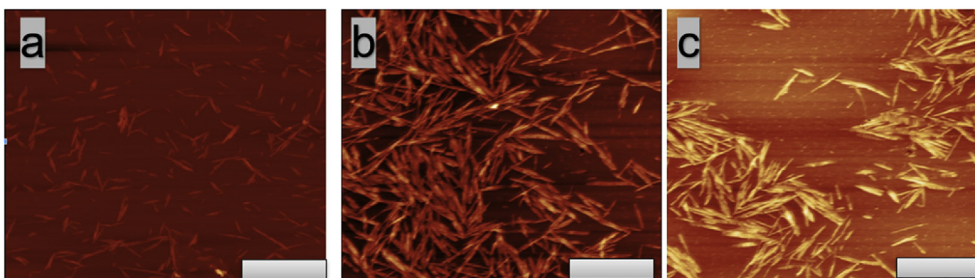


Fig. 4. AFM images of (a) neat CNCs; (b) Self-catalyzed modified CNCs; and (c) base-catalyzed modified CNCs; Scale bars are equal to 500 nm.

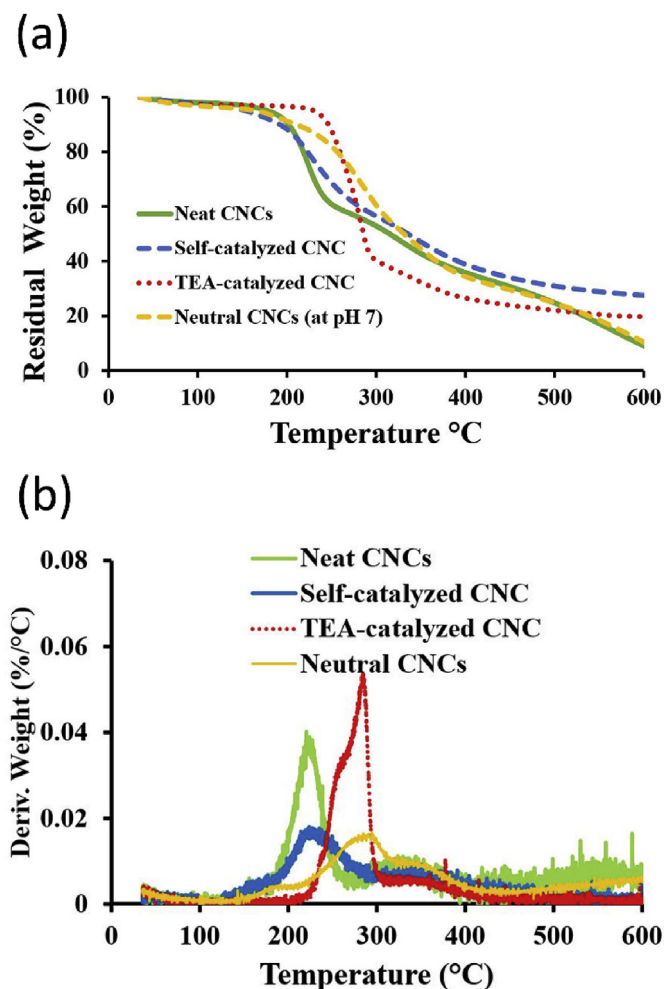


Fig. 5. (a) TGA thermograph of neat CNCs, neutral CNCs, self-catalyzed modified CNCs, and triethylamine (TEA) catalyzed modified CNCs; (b) DTG curve of neat CNCs and modified CNCs.

Zeta potential measurements of the neat CNCs and modified CNCs confirmed the presence of negative sulfate ions in the modified CNCs (Table 2). Both self-catalyzed CNCs and TEA-catalyzed CNCs had high negative zeta potentials confirming the modification reaction did not remove the sulfate groups. TEA-catalyzed CNCs had comparatively lower zeta potential (-32.3 ± 4.1) than self-catalyzed (-42.2 ± 5.2) and neat CNCs (-52.1 ± 14.2), which was possibly due to a higher hydrophobicity of the modified products hindering the adsorption of hydroxide ions on the CNC surface.

3.5. Changes in contact angle and wettability of the modified CNCs

The contact angles of the neat and modified CNCs were measured with water, ethylene glycol (EG) and diiodomethane (DIM) as liquid probes. At least three films were prepared, and three repetitions were made with each liquid. Table 3 shows the contact angle data. The surface of neat CNCs contains mostly OH rich (polar) surfaces, yet C–H rich (non-polar surface) are also present. The contact angle varies depending on the

Table 2
Zeta potential of CNC samples at pH 7.

Samples	Zeta potential (mV)
Neat CNCs	-52.1 ± 14.2
Self-catalyzed CNCs	-42.2 ± 5.2
TEA-catalyzed CNCs	-32.3 ± 4.1

proportion of each surface type exposed on the CNC film [53]. Bruel et al. reported that the CNC films made by oven casting were amphiphilic in nature [53], having both hydrophobic and hydrophilic sections exposed on the surface. With the polar liquid probes (water and EG), the contact angle increased with the modification of CNCs. The water contact angle of TEA-catalyzed CNC films is higher ($57.2 \pm 5.5^\circ$) than self-catalyzed CNC film ($43.1 \pm 3.2^\circ$) and neat CNC film ($25.9 \pm 4.1^\circ$). Contact angle of CNC films with EG followed a similar trend, indicating the increase in hydrophobicity and decrease in wettability with conversion of the Oxa-Michael addition. On the contrary, diiodomethane (DIM) showed an opposite trend; TEA-catalyzed CNC films had a lower contact angle ($23.0 \pm 1.5^\circ$) than the self-catalyzed ($35.5 \pm 0.4^\circ$) and neat CNC films ($41.6 \pm 3.3^\circ$). Thus, the contact angle of the nanoparticles revealed a direct relation of their hydrophobicity with reaction conversion.

3.6. Dispersibility of modified CNCs in organic medium

The dispersibility of the modified CNCs was tested by dispersing them in organic solvents, followed by the sonication until a stable dispersion was formed. Fig. 6 shows the dispersions of neat CNCs and modified CNCs in acetone, acetonitrile, and toluene. Based on visual inspection, all CNC samples appear aggregated in the organic solvents, although the base-catalyzed modified CNCs showed better dispersibility than the other two (Fig. 6a,b,c). This was further demonstrated by the TEA-catalyzed CNCs having higher UV–vis absorbance than the others. The relatively flat UV–vis spectra indicated significant scattering arising from aggregated or flocculated CNCs in suspension. Attachment of hydrophobic BnM on the CNC surface during modification process promoted hydrophobicity to the modified nanoparticles that helped to disperse them well in organic solvents. The increased dispersibility in organic liquids was not high, probably due to the existence of negatively charged sulfate groups and amphiphilic properties of the modified CNCs. The modified CNCs possessed both hydrophilic and hydrophobic groups on the surface which makes them suitable for applications like emulsions stabilizers, nanocomposite development, bionanomaterials, paper coating, solar cells, enhanced oil recovery, and underground CO₂ sequestration.

3.7. Sustainability

The reaction scheme of CNC with N-Benzylmaleimide (BnM) directly addresses six green chemistry principles: atom economy, less hazardous chemical synthesis, designing safer chemicals (products), use of renewable feedstocks, reduced derivatives, and inherently safer chemistry for accident prevention. It should be noted, there is no such thing as a 100% green chemical process. In the case of the method herein proposed, the reaction temperature of 70 °C could be further reduced in future work by creating or identifying different catalysts. However, the presented Oxa-Michael addition method is “greener” than other CNC modification routes as evidence by the application of 6 of the 12 green chemistry principles.

Atom economy refers to the mass of reactant atoms that are part of the final product according to the balanced reaction; hydroxyl addition to BnM had 100% atom economy. The mass efficiency (RME) of the modification reactions were calculated by using the method described by Constable et al. [54] and shown in Table S1. The RME of the self-catalyzed modification reaction run at 70 °C after 72 h, was calculated to be 81.93% and the RME of TEA-catalyzed reaction was 89.2%.

Table 3
Contact angle of CNC films on various liquid probes.

CNC films	Water	Ethylene Glycol (EG)	Diiodomethane (DIM)
Neat CNCs	25.9 ± 4.1	30.2 ± 2.2	41.6 ± 3.3
Self-catalyzed CNCs	43.1 ± 3.2	42.5 ± 3.1	35.5 ± 0.4
TEA-catalyzed CNCs	57.2 ± 5.5	52.3 ± 4.4	23.0 ± 1.5

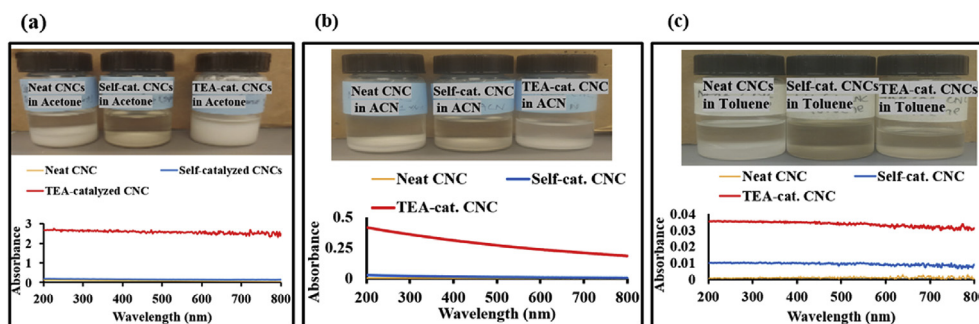


Fig. 6. Dispersions of neat CNCs, self-catalyzed CNCs and TEA-catalyzed CNCs and respective UV-Visible spectroscopy in (a) acetone; (b) acetonitrile (ACN); (c) Toluene.

Moreover, the low or limited toxicity of CNCs, DMSO, triethylamine and N-Benzylmaleimide, along with moderate reaction conditions addresses the less hazardous chemical synthesis principle. The toxicological data of the chemicals used in the modification reactions are provided in Table S2. TEA appears to have the largest toxicity among all components, yet it is used in catalytic amounts. The grafted CNC product is also expected to have a low toxicity while maintaining high performance, thus yielding a safer and efficient product. CNCs are obtained from plant-based renewable feedstocks, specifically SBSK pulp. No unnecessary protection, deprotection, or derivatization steps are performed, thereby reducing the use of derivatives. The chemistry is considered inherently safe, since the CNCs and BnM both have relatively low toxicity, low flammability, and do not undergo violent reactions under normal reaction or storage conditions. It must be noted that the low cost is an inherent part of sustainability; these principles must be applied while maintaining economical practicality. The safer reaction, low cost of chemicals, moderate reaction conditions, and lower accident risk are all expected to benefit the economics of a potential large-scale process.

4. Conclusion

In this study, surface modification of CNCs was achieved by the oxo-Michael addition of primary hydroxyl groups to N-Benzylmaleimide (BnM) to increase hydrophobicity and thermal stability. Overall, the grafting of BnM on the CNC surface improved the thermal stability and dispersibility in organic media. The increased hydrophobicity of the modified CNCs was corroborated by contact angle measurements. The TEA-catalyzed reaction showed a higher degree of modification than the self-catalyzed reaction. All the reactants used in the modification of CNCs had low-toxicity, improving the greenness of modified CNCs. The modification reaction featured 100% atom economy, high reaction mass efficiency (>80% in both reaction routes), reduced derivatives, and safer chemistry for accident prevention. The CNCs were collected from a renewable source and all the chemicals used in the process were inexpensive, improving the economic viability of the process. The hydrophobized CNCs were prepared by attaching BnM via chemically and thermally stable ether linkages. The prepared CNCs can potentially be used to reinforce polymer nanocomposites and other applications requiring elevated temperatures like solar cells, CO₂ underground sequestration, or to enhance chemical processes in extreme environments.

CRedit authorship contribution statement

Mohammad Jahid Hasan: Investigation, Methodology, Formal analysis, Data curation, Writing – original draft, preparation, Visualization. **Ashley E. Johnson:** Investigation. **Esteban E. Ureña-Benavides:** Conceptualization, Methodology, Resources, Writing – review & editing, Project administration.

Declaration of competing interest

The authors declare that they have no known competing financial interests or personal relationships that could have appeared to influence the work reported in this paper.

Acknowledgement

We thank Dr. Nehal Abu-Lail for the use of the contact angle analyzer, Dr. Jared Delcamp for the NMR use, and Drs Xiaobing Li and Ahmed Al-Ostaz for TGA and FTIR use. We thank the University of Mississippi and the University of Texas at San Antonio for financial support.

Appendix A. Supplementary data

Supplementary data to this article can be found online at <https://doi.org/10.1016/j.crgsc.2021.100081>.

References

- [1] Y. Kojima, A. Usuki, M. Kawasumi, A. Okada, T. Kurauchi, O. Kamigaito, Synthesis of nylon 6–clay hybrid by montmorillonite intercalated with ϵ -caprolactam, *J. Polym. Sci. Polym. Chem.* 31 (1993) 983–986, <https://doi.org/10.1002/pola.1993.080310418>.
- [2] M.A.S. Azizi Samir, F. Alloin, A. Dufresne, Review of recent research into cellulosic whiskers, their properties and their application in nanocomposite field, *Biomacromolecules* 6 (2005) 612–626, <https://doi.org/10.1021/bm0493685>.
- [3] Y. Habibi, L.A. Lucia, O.J. Rojas, Cellulose nanocrystals: chemistry, self-assembly, and applications, *Chem. Rev.* 110 (2010) 3479–3500, <https://doi.org/10.1021/cr900339w>.
- [4] F.H.A. Rodrigues, C. Spagnol, A.G.B. Pereira, A.F. Martins, A.R. Fajardo, A.F. Rubira, E.C. Muniz, Superabsorbent hydrogel composites with a focus on hydrogels containing nanofibers or nanowhiskers of cellulose and chitin, *J. Appl. Polym. Sci.* 131 (2014), <https://doi.org/10.1002/app.39725>.
- [5] M. Mariano, N.E. Kissi, A. Dufresne, Cellulose nanocrystals and related nanocomposites: review of some properties and challenges, *J. Polym. Sci. B Polym. Phys.* 52 (2014) 791–806, <https://doi.org/10.1002/polb.23490>.
- [6] Y. Habibi, Key advances in the chemical modification of nanocelluloses, *Chem. Soc. Rev.* 43 (2014) 1519–1542, <https://doi.org/10.1039/C3CS60204D>.
- [7] A.W. Carpenter, C.-F. de Lannoy, M.R. Wiesner, Cellulose nanomaterials in water treatment Technologies, *Environ. Sci. Technol.* 49 (2015) 5277–5287, <https://doi.org/10.1021/es506351r>.
- [8] S.Y. Ooi, I. Ahmad, MohdC.I.M. Amin, Cellulose nanocrystals extracted from rice husks as a reinforcing material in gelatin hydrogels for use in controlled drug delivery systems, *Ind. Crop. Prod.* 93 (2016) 227–234, <https://doi.org/10.1016/j.indcrop.2015.11.082>.
- [9] S. Parajuli, A.L. Dorris, C. Middleton, A. Rodriguez, M.O. Haver, N.I. Hammer, E. Ureña-Benavides, Surface and interfacial interactions in dodecane/brine pickering emulsions stabilized by the combination of cellulose nanocrystals and emulsifiers, *Langmuir* 35 (2019) 12061–12070, <https://doi.org/10.1021/acs.langmuir.9b01218>.
- [10] L. Bai, S. Lv, W. Xiang, S. Huan, D.J. McClements, O.J. Rojas, Oil-in-water Pickering emulsions via microfluidization with cellulose nanocrystals: 1. Formation and stability, *Food Hydrocolloids* 96 (2019) 699–708, <https://doi.org/10.1016/j.foodhyd.2019.04.038>.
- [11] B. Hutton-Prager, M.M. Khan, C. Gentry, C.B. Knight, A.K.A. Al-Abri, Thermal barrier enhancement of calcium carbonate coatings with nanoparticle additives, and their effect on hydrophobicity, *Cellulose* 26 (2019) 4865–4880, <https://doi.org/10.1007/s10570-019-02426-9>.

- [12] K. Yuwawech, J. Wootthikanokkhan, S. Wanwong, S. Tanpichai, Polyurethane/esterified cellulose nanocrystal composites as a transparent moisture barrier coating for encapsulation of dye sensitized solar cells, *J. Appl. Polym. Sci.* 134 (2017) 45010, <https://doi.org/10.1002/app.45010>.
- [13] K.B. Azouz, E.C. Ramires, W. Van Den Fonteyne, N.E. Kissi, A. Dufresne, A simple method for the melt extrusion of cellulose nano-crystal reinforced hydrophobic polymer, *ACS Macro Lett.* 1 (2011) 236–240.
- [14] R.C. Aadland, T.D. Jakobsen, E.B. Heggset, H. Long-Sanouiller, S. Simon, K.G. Paso, K. Syverud, O. Torsæter, High-temperature core flood investigation of nanocellulose as a green additive for enhanced oil recovery, *Nanomaterials* 9 (2019), <https://doi.org/10.3390/nano9050665>.
- [15] E.E. Ureña-Benavides, G. Ao, V.A. Davis, C.L. Kitchens, Rheology and phase behavior of lyotropic cellulose nanocrystal suspensions, *Macromolecules* 44 (2011) 8990–8998, <https://doi.org/10.1021/ma201649f>.
- [16] E.E. Ureña-Benavides, P.J. Brown, C.L. Kitchens, Effect of jet stretch and particle load on cellulose Nanocrystal–Alginate nanocomposite fibers, *Langmuir* 26 (2010) 14263–14270, <https://doi.org/10.1021/la102216v>.
- [17] J.R. Capadona, O. Van Den Berg, L.A. Capadona, M. Schroeter, S.J. Rowan, D.J. Tyler, C. Weder, A versatile approach for the processing of polymer nanocomposites with self-assembled nanofibre templates, *Nat. Nanotechnol.* 2 (2007) 765–769, <https://doi.org/10.1038/nnano.2007.379>.
- [18] J.R. Capadona, K. Shanmuganathan, S. Trittschuh, S. Seidel, S.J. Rowan, C. Weder, Polymer nanocomposites with nanowhiskers isolated from microcrystalline cellulose, *Biomacromolecules* 10 (2009) 712–716, <https://doi.org/10.1021/bm8010903>.
- [19] P.K. Annamalai, K.L. Dagnon, S. Monemian, E.J. Foster, S.J. Rowan, C. Weder, Water-responsive mechanically adaptive nanocomposites based on styrene-butadiene rubber and cellulose nanocrystals—processing matters, *ACS Appl. Mater. Interfaces* 6 (2014) 967–976, <https://doi.org/10.1021/am404382x>.
- [20] N. Lin, J. Huang, A. Dufresne, Preparation, properties and applications of polysaccharide nanocrystals in advanced functional nanomaterials: a review, *Nanoscale* 4 (2012) 3274–3294, <https://doi.org/10.1039/c2nr30260h>.
- [21] A. Dufresne, *Nanocellulose: from Nature to High Performance Tailored Materials*, Walter de Gruyter GmbH, 2012.
- [22] S. Iwamoto, A. Isogai, T. Iwata, Structure and mechanical properties of wet-spun fibers made from natural cellulose nanofibers, *Biomacromolecules* 12 (2011) 831–836, <https://doi.org/10.1021/bm101510r>.
- [23] C. Goussé, H. Chanzy, M.L. Cerrada, E. Fleury, Surface silylation of cellulose microfibrils: preparation and rheological properties, *Polymer* 45 (2004) 1569–1575, <https://doi.org/10.1016/j.polymer.2003.12.028>.
- [24] H. Liimatainen, M. Visanko, J. Sirviö, O. Hormi, J. Niinimäki, Sulfonated cellulose nanofibrils obtained from wood pulp through regioselective oxidative bisulfite pre-treatment, *Cellulose* 20 (2013) 741–749, <https://doi.org/10.1007/s10570-013-9865-y>.
- [25] S. Ifuku, M. Nogi, K. Abe, K. Handa, F. Nakatsubo, H. Yano, Surface modification of bacterial cellulose nanofibers for property enhancement of optically transparent Composites: dependence on acetyl-group DS, *Biomacromolecules* 8 (2007) 1973–1978, <https://doi.org/10.1021/bm070113b>.
- [26] B. Braun, J.R. Dorgan, Single-step method for the isolation and surface functionalization of cellulosic nanowhiskers, *Biomacromolecules* 10 (2009) 334–341, <https://doi.org/10.1021/bm801117>.
- [27] D. Morantes, E. Muñoz, D. Kam, O. Shoseyov, Highly charged cellulose nanocrystals applied as A water treatment flocculant, *Nanomaterials* 9 (2019) 272, <https://doi.org/10.3390/nano9020272>.
- [28] A. Bendahou, A. Hajlane, A. Dufresne, S. Boufi, H. Kaddami, Esterification and amidation for grafting long aliphatic chains on to cellulose nanocrystals: a comparative study, *Res. Chem. Intermed.* 41 (2015) 4293–4310, <https://doi.org/10.1007/s11164-014-1530-z>.
- [29] X. Yang, E.D. Cranston, Chemically cross-linked cellulose nanocrystal aerogels with shape recovery and superabsorbent properties, *Chem. Mater.* 26 (2014) 6016–6025, <https://doi.org/10.1021/cm502873c>.
- [30] E. Lam, K.B. Male, J.H. Chong, A.C.W. Leung, J.H.T. Luong, Applications of functionalized and nanoparticle-modified nanocrystalline cellulose, *Trends Biotechnol.* 30 (2012) 283–290, <https://doi.org/10.1016/j.tibtech.2012.02.001>.
- [31] C.F. Nising, S. Bräse, Recent developments in the field of oxa-Michael reactions, *Chem. Soc. Rev.* 41 (2012) 988–999, <https://doi.org/10.1039/C1CS15167C>.
- [32] S.-H. Guo, S.-Z. Xing, S. Mao, Y.-R. Gao, W.-L. Chen, Y.-Q. Wang, Oxa-Michael addition promoted by the aqueous sodium carbonate, *Tetrahedron Lett.* 55 (2014) 6718–6720, <https://doi.org/10.1016/j.tetlet.2014.10.019>.
- [33] M. Barbero, S. Cadamuro, S. Dughera, O-benzenedisulfonamide as a reusable brønsted acid catalyst for hetero-michael reactions, *Synth. Commun.* 43 (2013) 758–767, <https://doi.org/10.1080/00397911.2011.614834>.
- [34] T.C. Wabnitz, J.B. Spencer, A general, brønsted acid-catalyzed hetero-michael addition of nitrogen, oxygen, and sulfur nucleophiles, *Org. Lett.* 5 (2003) 2141–2144, <https://doi.org/10.1021/ol034596h>.
- [35] Y.-M. Hong, Z. Shen, X. Hu, W. Mo, X.-F. He, B. Hu, N. Sun, Acid-catalyzed intramolecular oxa-Michael addition reactions under solvent-free and microwave irradiation conditions, <https://doi.org/10.3998/ark.5550190.0010.e14>, 2010.
- [36] P. Anastas, N. Eghbali, Green chemistry: principles and practice, *Chem. Soc. Rev.* 39 (2010) 301–312, <https://doi.org/10.1039/B918763B>.
- [37] J. Tang, J. Sisler, N. Grishkewich, K.C. Tam, Functionalization of cellulose nanocrystals for advanced applications, *J. Colloid Interface Sci.* 494 (2017) 397–409, <https://doi.org/10.1016/j.jcis.2017.01.077>.
- [38] A.G. Cunha, J.-B. Mougel, B. Cathala, L.A. Berglund, I. Capron, Preparation of double pickering emulsions stabilized by chemically tailored nanocelluloses, *Langmuir* 30 (2014) 9327–9335, <https://doi.org/10.1021/la5017577>.
- [39] G. Sèbe, F. Ham-Pichavant, G. Pecastaings, Dispersibility and emulsion-stabilizing effect of cellulose nanowhiskers esterified by vinyl acetate and vinyl cinnamate, *Biomacromolecules* 14 (2013) 2937–2944, <https://doi.org/10.1021/bm400854n>.
- [40] J. Shin, S. Nouranian, E.E. Ureña-Benavides, A.E. Smith, Dynamic mechanical and thermal properties of cellulose nanocrystal/epoxy nanocomposites, *Green Mater.* 5 (2017) 123–134, <https://doi.org/10.1680/jgrma.17.00005>.
- [41] S.N. Molnes, A. Mamonov, K.G. Paso, S. Strand, K. Syverud, Investigation of a new application for cellulose nanocrystals: a study of the enhanced oil recovery potential by use of a green additive, *Cellulose* 25 (2018) 2289–2301, <https://doi.org/10.1007/s10570-018-1715-5>.
- [42] S. Parajuli, L.A. Prater, T. Heath, K.A. Green, W. Moyer, B. Hutton-Prager, E.E. Ureña-Benavides, Cellulose nanocrystal-stabilized dispersions of CO₂, heptane, and perfluorooctane at elevated temperatures and pressures for underground CO₂ sequestration, *ACS Appl. Nano Mater.* 3 (2020) 12198–12208, <https://doi.org/10.1021/acsnano.0c02653>.
- [43] D.G. Gray, Transcrystallization of polypropylene at cellulose nanocrystal surfaces, *Cellulose* 15 (2008) 297–301, <https://doi.org/10.1007/s10570-007-9176-2>.
- [44] T. Abitbol, E. Kloser, D.G. Gray, Estimation of the surface sulfur content of cellulose nanocrystals prepared by sulfuric acid hydrolysis, *Cellulose* 20 (2013) 785–794, <https://doi.org/10.1007/s10570-013-9871-0>.
- [45] O. van den Berg, J.R. Capadona, C. Weder, Preparation of homogeneous dispersions of tunicate cellulose whiskers in organic solvents, *Biomacromolecules* 8 (2007) 1353–1357, <https://doi.org/10.1021/bm061104q>.
- [46] W.M. Haynes, *CRC Handbook of Chemistry and Physics*, 96th Edition, CRC Press, 2015.
- [47] L. Tang, C. Weder, Cellulose whisker/epoxy resin nanocomposites, *ACS Appl. Mater. Interfaces* 2 (2010) 1073–1080, <https://doi.org/10.1021/am900830h>.
- [48] M. Roman, Toxicity of cellulose nanocrystals: a review, *Ind. Biotechnol.* 11 (2015) 25–33, <https://doi.org/10.1089/ind.2014.0024>.
- [49] P. Dhar, A. Kumar, V. Katiyar, Magnetic cellulose nanocrystal based anisotropic polylactic acid nanocomposite films: influence on electrical, magnetic, thermal, and mechanical properties, *ACS Appl. Mater. Interfaces* 8 (2016) 18393–18409, <https://doi.org/10.1021/acsnano.6b02828>.
- [50] E.Y. Wardhono, H. Wahyudi, S. Agustina, F. Oudet, M.P. Pinem, D. Clause, K. Saleh, E. Guénin, Ultrasonic irradiation coupled with microwave treatment for eco-friendly process of isolating bacterial cellulose nanocrystals, *Nanomaterials* 8 (2018) 859, <https://doi.org/10.3390/nano8100859>.
- [51] H. Kargarzadeh, I. Ahmad, I. Abdullah, A. Dufresne, S.Y. Zainudin, R.M. Sheltami, Effects of hydrolysis conditions on the morphology, crystallinity, and thermal stability of cellulose nanocrystals extracted from kenaf bast fibers, *Cellulose* 19 (2012) 855–866, <https://doi.org/10.1007/s10570-012-9684-6>.
- [52] D. Bondeson, K. Oksman, Dispersion and characteristics of surfactant modified cellulose whiskers nanocomposites, *Compos. Interfac.* 14 (2007) 617–630, <https://doi.org/10.1163/156855407782106519>.
- [53] C. Bruel, S. Queffeuilou, P.J. Carreau, J.R. Tavares, M.-C. Heuzey, Orienting cellulose nanocrystal functionalities tunes the wettability of water-cast films, *Langmuir* 36 (2020) 12179–12189, <https://doi.org/10.1021/acs.langmuir.0c01799>.
- [54] D.J. Constable, A.D. Curzons, V.L. Cunningham, Metrics to 'green' chemistry—which are the best? *Green Chem.* 4 (2002) 521–527.